Nanoscale

Accepted Manuscript

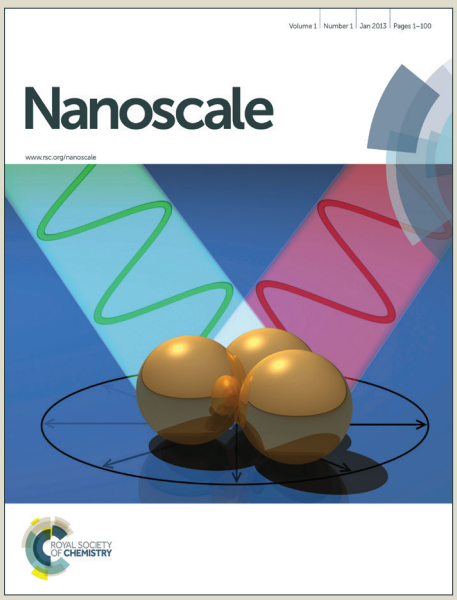

ROYAL SOCIETY OF CHEMISTRY

www.rsc.org/nanoscale

Nanoscale

RSCPublishing

ARTICLE

Facile synthesis of gold nanoworms with tunable length and aspect ratio through oriental attachment of nanoparticles

Waqqar Ahmed,[ab] Christian Glass[a] and Jan M. van Ruitenbeek*[a]

Cite this: DOI: 10.1039/x0xx00000x

Received 00th January 2012,
Accepted 00th January 2012

DOI: 10.1039/x0xx00000x

www.rsc.org/

We report a seedless protocol based on the oriental attachment of nanoparticles for the synthesis of Au nanoworms (NWs). NWs are grown by reducing $HAuCl_4$ with ascorbic acid (AA) in high pH reaction medium and in the presence of growth directional agents, cetyltrimethylammonium bromide (CTAB) and $AgNO_3$. . Although we have used the same reducing and growth directional agents as typically used for the synthesis of Au nanorods, the growth mechanism of NWs is markedly different from that of nanorods. Instead of the anisotropic growth of seed particles, the NWs grow through oriental attachment of nanoparticles. By varying different reaction parameters we have seen that the length of NWs can be controlled from tens of nanometers to a micrometer. Furthermore, the aspect ratio (AR) can be tuned from 2 to 30. This is almost the whole range of AR and length for Au nanorods so far achieved with seed-mediated multiple step synthesis protocols.

Introduction

Nobel metal nanoparticles have attracted enormous attention recently owing to their interesting optical properties.[1-8] The collective excitation of electrons under the influence of electromagnetic waves, leads to interesting absorption and scattering properties. The nanoparticles have a characteristic signature plasmon peak, which is very sensitive to their size and shape.[5]

For anisotropic nanoparticles, there are multiple plasmon peaks owing to their shape anisotropy. For rod-shaped nanoparticles there are two plasmon peaks associated with the plasmon excitations along the width and along the length of nanorods.[9,10] Non-centrosymetric nanoparticles show several plasmon resonances arising from the asymmetry of particle's shape.[11,12] For instance, L-shape nanoparticles can have as many as four plasmon peaks.[11] Furthermore, it has been shown that slight changes in ordering of non-centrosymetric metallic L-shaped nanoparticles can have a remarkable influence on the optical response.[13] These properties make non-centrosymmetric nanoparticles potential candidates for sensing applications.

For the high-yield synthesis of anisotropic Au nanoparticles, seed-mediated growth protocols are very well established.[14-17] The methods invariably encompass multiple steps. First, spherical Au nanoparticles (2-3 nm) are formed, usually by reducing Au ions by a strong reducing agent such as $NaBH_4$. These seeds are than added to the growth solution that commonly contains Au ions, growth directional agents (CTAB and $AgNO_3$) and a mild reducing agent (AA). It is widely believed that AA reduces Au (III) to Au(I) in the growth solution.[14,15] Therefore, the addition of the seed particles is essential as they provide catalytic effect for complete reduction of Au. However, Jana has demonstrated that when, in addition to ascorbic acid, a strong reducing agent (such as $NaBH_4$) is used in the growth solution, the growth of Au nanorods can occur without seeds.[18]

The seed-mediated protocol for the synthesis of nanorods has been modified to synthesize more complex shapes such as nanostars, nanoflowers, nanotripods, nanofruits and nanobelts.[19-32] Recently, there was also a report on the synthesis of high AR ultrathin twisted Au nanowires on the substrate. He *et al.* used the seed mediated method to grow the nanowires directly on the substrates.[33] However, their method required various steps such as synthesis of Au seeds, functionalization of substrate, deposition of seeds on the substrate, growth of the wires from seeds and finally removal of wires from the substrate. The authors did not obtained nanowires in the solution using the same conditions. A solution based synthesis of twisted Au nanowires has been demonstrated by Zhu *et al*.[34] However, their nanowires are hydrophobic which restricts their use in aqueous medium. Furthermore, the nanowires are ultra-long and have extreme ARs. While the ultra-thin, ultra-long nanowires may have interesting electron transport properties (that makes them quite useful for nanoelectronics), their optical properties are of rather limited interest. The longitudinal plasmon peak for such wires lies at

very low energies due to their high AR.[9] Therefore, the synthesis of low AR (< 30) non-centrosymmetric nanoparticles will be very useful for numerous optics-based applications. In this paper we describe the synthesis of low AR worm-shaped Au nanoparticles using a one-step synthesis protocol. We show that worm-shaped gold nanoparticles can be prepared by reducing Au ions with AA. In contrast to the previous reports, the presence of seeds or a strong reducing agent is not required for the synthesis of nanoparticles. The NWs grow through oriental attachment of nanoparticles in the reaction medium. We demonstrate that the length and AR of NWs can be tuned in a wide range simply by tuning the concentrations of various reactants. Our method is exceptionally simple and only requires mixing of a few chemicals.

Table 1: The concentration of reactants for various samples, and the measured values for the length, AR, and the yield (percentage of the NWs in the final product).

Fig. no.	CTAB (M)	$HAuCl_4$ (mM)	AA (mM)	NaOH (mM)	$AgNO_3$ (mM)	Length (nm)	AR	Yield
1a	0.2	0.25	0.27	2	0.05	200±40	8±1.4	45%
1b	0.2	0.25	0.27	2	0.1	1200±400	30±10	>90%
1c	0.2	0.25	0.27	2	0.2	600±200	17±7	>90%
1d	0.2	0.25	0.27	2	0.3	190±20	21±3	>90%
1e	0.2	0.25	0.27	2	0.35	150±20	13±2	>90%
1f	0.2	0.25	0.27	2	0.45	120±20	8±3	>90%
2a	0.1	0.25	0.27	2	0.3	40±10	3.6±0.9	80%
2b	0.05	0.25	0.27	2	0.3	19±4	2.2±0.6	75%
2c	0.2	0.15	0.17	2	0.3	110±20	5.4±0.9	70%
2d	0.2	0.25	0.27	2.5	0.3	70±20	7±2	>90%
2e	0.2	0.25	0.27	1.5	0.3	180±50	15±6	>90%
2f	0.2	0.25	0.27	0	0.3			0%

Experimental

Materials

All chemicals were purchased from Sigma-Aldrich. All reagents were used as-received, without any further purification. Millipore water (resistivity =18.2 MΩ cm) was used for making all solutions.

Synthesis of Au NWs

In order to synthesize NWs, $HAuCl_4$ was added in a CTAB solution and was stirred until a clear yellowish solution was obtained. In this solution, ascorbic acid (AA) solution was added immediately under stirring. The addition of ascorbic acid caused the yellowish solution to become colourless. Next, NaOH was added. If the solution is left at this stage it will slowly change colour. Therefore, addition of NaOH was immediately followed by addition of $AgNO_3$. This caused a very fast colour change of the solution from colourless to dark brown, indicating the formation of NWs. The solution was left undisturbed overnight at 26°C. Table 1 depicts the concentrations of various chemicals used to synthesize NWs of different lengths and aspect ratios.

Characterization

The imaging of NWs was done by a Nova NanoSEM 200 scanning electron microscope (SEM) and Philips CM 300ST Transmission Electron Microscope (TEM). The optical spectrum was obtained by Ocean Optics spectrometer.

All samples were centrifuged twice to remove excess CTAB before imaging. For TEM and SEM analysis, drop-casting of NW solution was done on a carbon grid and Si/SiO_2 wafer, respectively.

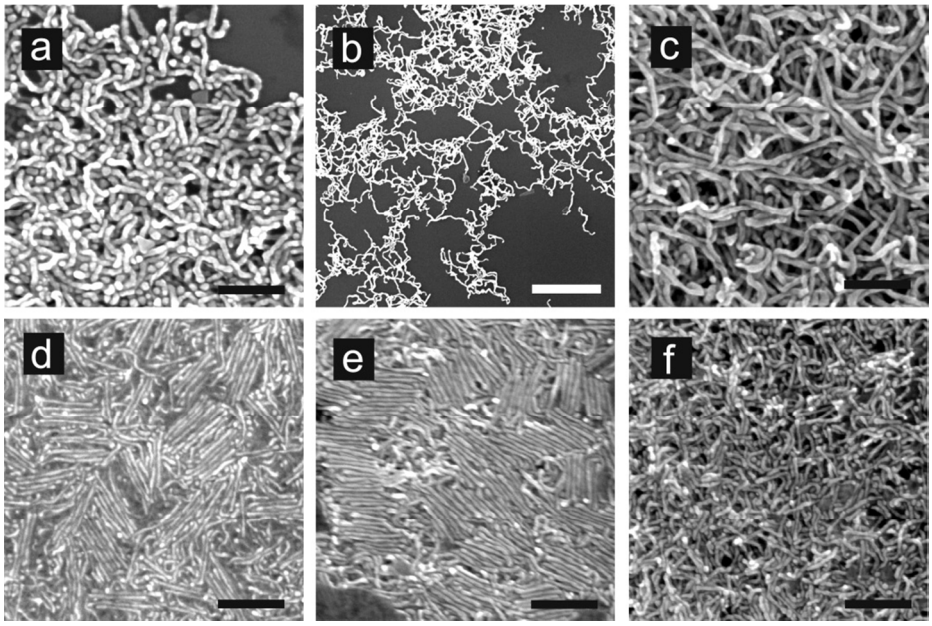

Fig. 1 Au NWs synthesized with various $AgNO_3$ concentrations ($AgNO_3$ concentration increases from a to f). The black and white scales bars amount to 200 nm and 1 μm, respectively.

Results and discussion

Fig. 1a shows a scanning electron microscope (SEM) image of NWs prepared with CTAB, $HAuCl_4$, AA, NaOH and $AgNO_3$ concentrations of 0.2 M, 0.25 mM, 0.27 mM, 2 mM and 0.05 mM, respectively. The length of NWs is 200±40 nm and their AR amounts to 8±1.4. As evident from the SEM image, particles have a worm-like shape. The yield of worm-shaped NWs is only 45% in this case. Increasing the $AgNO_3$ concentration to 0.1 mM gives a much higher (>90%) yield of NWs. The length and AR of NWs increases as well, as can be seen in Fig. 1b (note the different scale bar). Further increase in Ag ion concentration to 0.2 mM results in a decrease in the length of the NWs, as shown in the SEM image of Fig. 1c. For an Ag ion concentration of 0.3 mM the NWs are least polydisperse (Fig. 1d). Ag ion concentrations higher than 0.3 mM result in a larger dispersion in particle size and AR (Fig. 1d-f and Table 1). Overall, with the exception of Fig. 1a (where the yield of NWs is markedly low), the length of NWs decrease with increase in $AgNO_3$ concentration (Fig. 3).

The length and AR of NWs can also be tuned by controlling the concentration of the surfactant (CTAB) in solution. Figure 2a depicts the NWs prepared at a lower CTAB concentration (0.1 M), while keeping other reaction conditions the same as used for preparing NWs in Figure 1d. In this case the NWs have a much smaller length

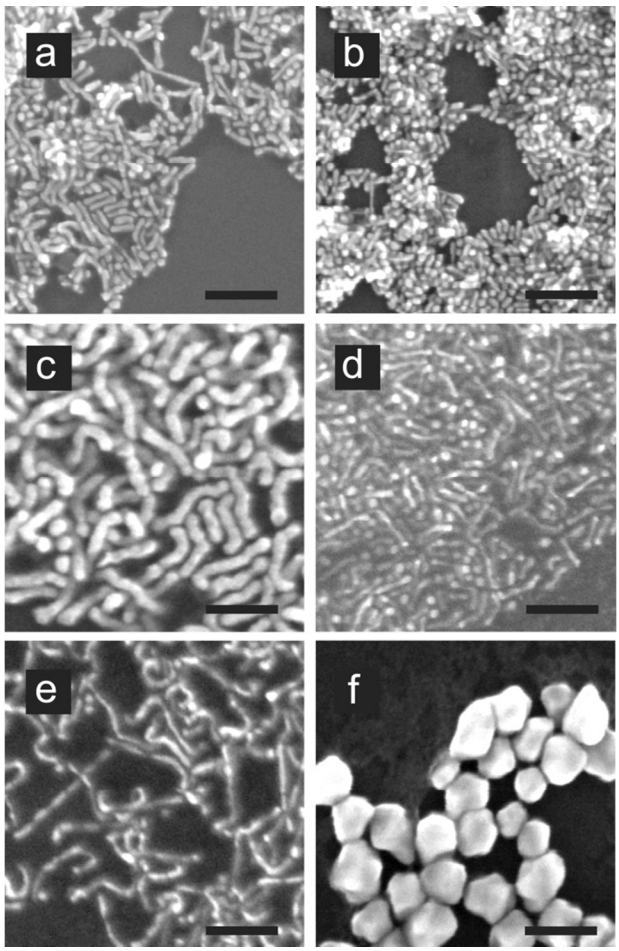

Fig. 2 Au NWs synthesized by the CTAB concentrations of (a) 0.1 M and (b) 0.05 M; $HAuCl_4$ concentration of (c) 0.15M; NaOH concenrations of (d) 2.5 mM, (e) 1.5 mM and (f) 0 mM. The rest of the reactants concentrations are same as used for NWS of Fig. 1d. The scale bar is 100 nm.

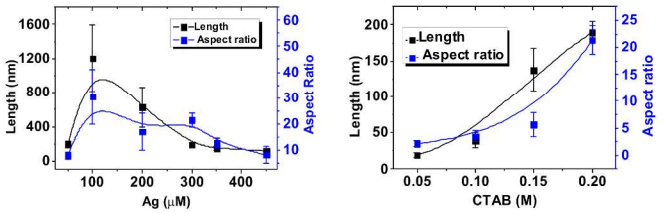

Fig. 3 Change in the length and aspect ratio of NWs with Ag (left) and CTAB (right) concentrations.

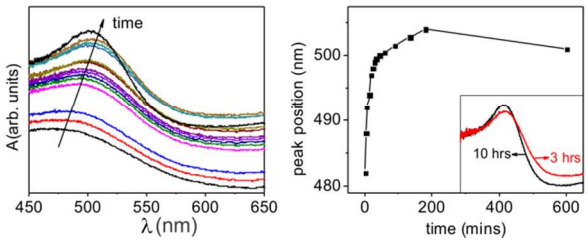

Fig. 4 Growth evolution of Au NWs. (a) Optical spectra recorded at different times of growth. (b) Low energy plasmon peak position for NWs as a function of time during the growth. Inset in b shows a comparison of the plasmon peak after 3 and 10 hours of growth time.

and AR. A further decrease in CTAB concentration to 0.05M leads to ultra-small NWs (19±4 nm in length and 2.2±0.6 in AR). Therefore, the length and aspect ratio of NWs increases with increase in CTAB concentration in reaction medium (Figure 3).

Similarly, the concentrations of $HAuCl_4$, NaOH, and AA also have considerable influence on the yield and morphology of NWs. For example, changing the concentration of Au ions (while keeping Au:AA at 1:1.1) give relatively thicker NWs (Fig. 2c Table 1), compared to reference NWs (Fig. 1d). Moreover, changing the concentration of NaOH in solution also markedly affects the size, morphology and aspect ratio of the NWs (Fig. 2 d-f and Table 1). Consequently, the length of NWs can be tuned from 18 nm to 1200 nm and their AR can be tuned from 2 to 30 by varying the concentration of various reactants.

The reaction mechanism for the synthesis of anisotropic Au nanoparticles in the presence of Ag ions, CTAB and AA is still under debate. Chen *et al.* used X-ray absorption spectroscopy to show that the addition of CTAB in a $HAuCl_4$ solution causes ligand exchange and chloride ions in the Au precursor are replaced by bromine ions.[35] They also pointed out that under normal pH conditions (i.e. in absence of NaOH in solution) the addition of AA in a solution containing Au^{+3} ions and CTAB leads to reduction of Au ions from the +3 to the 0 oxidation state, leading to the formation of the so-called Au_{13} clusters.[35] These clusters are surrounded by CTAB molecules, which stops them from agglomerating. In their experiments, once the nucleation seed particles are added in this solution these Au_{13} clusters attach to the seeds, leading to the growth of nanorods. However, this interpretation is in conflict with some other reports that suggest that AA is a weak reducing agent and can only reduce Au ions from the +3 to the +1 oxidation state.[14,15] On the other hand, the presence of NaOH in the solution is known to enhance the reducing power of AA,[16] enabling it to reduce the Au completely.

Similarly, various mechanisms for the role of Ag in the growth of anisotropic Au nanoparticles have been suggested. These include, facet-specific deposition of AgBr, under-potential deposition of Ag on various facets, and formation of a $CTA^+AgBr_2^-$ complex.[14,15,36,37] In our case the colour of the solution changed rapidly (from colorless to brown) with the addition of $AgNO_3$. This seems to suggest that Ag ions play a role in inducing the nucleation process. In order to verify whether this only happens in a high-pH reaction medium, we carried out a control experiment in which no NaOH was added in solution. Under normal pH conditions, with addition of Ag ions there was still a rapid color change indicating the formation of Au nanoparticles. However, only nanoparticles with AR's of nearly 1 were obtained in this case (Fig. 2f). Our results are consistent with the observations by Sau *et al.*,[38] who reported for the seed-mediated growth method that nucleation occurs even in the absence of seeds, when Ag is added after the addition of AA in solution. This also confirms that AA, even under normal pH conditions can reduce Au from the +3 to the 0 oxidation state.

In order to study the growth evolution of NWs, we recorder their optical spectra during the growth. The high energy plasmon peak was observed as a function of time. Similar to nanorods, the high energy plasmon peak's position for NWs depends upon the width of NWs.[9] Furthermore, the width of the peak is indicative of the polydispersity in particle's width (both, within one NW and between NWs). Fig. 4a shows the spectra at various times of growth. The intensity of the peak increases with the passage of time. This is due to the increase in the size and concentration of NWs with time. The plasmon peak position also changes with time. The initial red-shift is due to the increase in the width of the growing Au nuclei and NWs. However, after a few hours of growth the plasmon peak shifts a little to the blue. More importantly, at this stage the width of the plasmon peak is markedly reduced (see inset of Fig. 4b), indicating improvement in uniformity of the width of NW across its length.

Based on the above observations and discussion, we propose a mechanism for the formation of the NWs (Scheme 1). When $HAuCl_4$ is added in a CTAB solution, Cl^- ions are replaced by the Br^- ions provided by the surfactant. With addition of AA, Au ions in solution reduce from the +3 to the 0 oxidation state, leading to the formation of Au_{13} clusters.[35] These clusters cannot agglomerate to initiate nucleation of Au nanoparticles as they are surrounded by CTAB molecules. We believe that addition of Ag ions disturbs the ligand's shell surrounding the Au_{13} clusters and leads to the nucleation of metallic Au. Once the nuclei start growing they will be influenced by the 'zipping effect' of the CTAB bilayer.[16] The surfactant, CTAB, due to its larger head group has a better adhesion to the high energy {100} and {110} facets rather than the closely packed low energy {111} facet.[14] This anisotropic attachment of CTAB, combined with the fact that CTAB has a positive charge after losing the Br contour ion, leads to the generation of electrostatic forces among the growing nanoparticles. These electrostatic forces results in end-to-end adhering of particles rather than side-by-side leading to the formation of NWs. The role of electrostatic interactions in driving the assembly is also supported by the fact that the length of NWs increases by increasing the concentration of CTAB surfactant in the solution (Fig. 3). Higher concentration of CTAB in solution means better attachment of the CTAB molecules on the surface of growing nanoparticles, which in turn leads to stronger electrostatic interactions. Once the growth of NWs stops, the second step is the smoothening of their surface by mass redistribution, which is presumably driven by the reduction of the surface energy and surface defects.[39] This smoothening of the surface is seen in the reduction of plasmon peak width after a certain growth time, as discussed above (Fig. 4b). The surface of the NWs does not become completely smoothened and a neck remains at the particle junctions, as evident from the TEM images (Fig. 5). The growth of NWs in our case is

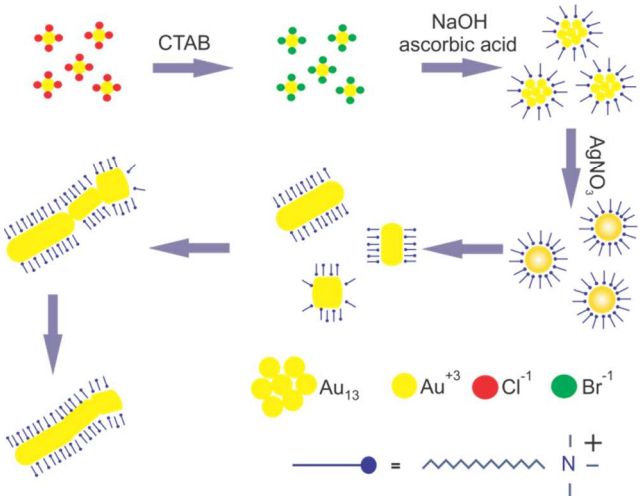

Scheme 1. Growth mechanism of NWs.

similar to the earlier reported growth of Pt_3Fe nanorods.[39] Liao *et al.* used in situ TEM analysis of the growth of Pt_3Fe nanorods by oriented attachment of nanoparticles driven by the dipolar forces.[39]

Support for the oriented attachment mechanism in our case can also be obtained from the transmission election microscope (TEM) images shown in Fig. 5. The images in Fig. 5(a,b) clearly indicate that the NWs are made up of a number of differently oriented domains. The red dotted curves represent the approximate boundaries of domains that, we propose, have started from particles that became attached in forming the NW. Fig. 5c shows a high magnification TEM image of the joint region in a NW. It is evident from the TEM image that the two sections at either end of the joint have different crystal orientations. We conclude that the NW is

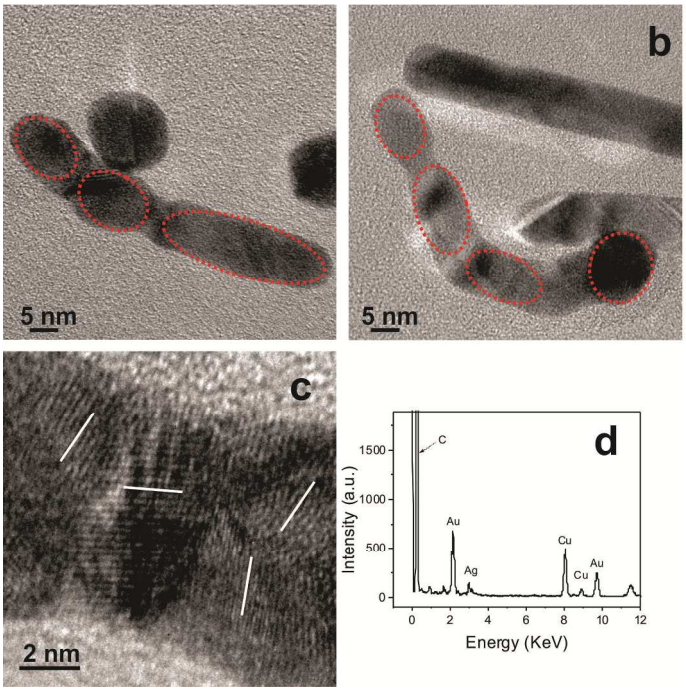

Fig. 5 (a, b) TEM image of the NWs. The red doted curves indicate regions representing different domains, presumably originating from particles that fused together to from the NW. (c) High resolution TEM image of the joint region of a NW. The white lines show atomic lattice directions. (d) EDS spectra of the NW shown in b.

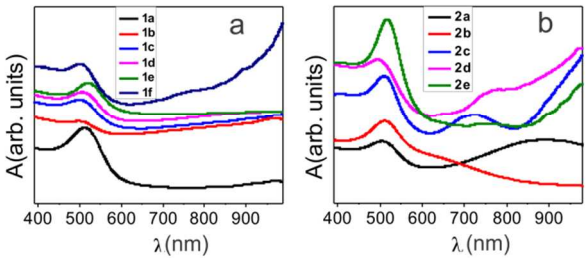

Fig. 6 (a) Optical spectra of NWs of Fig. 1(a-f). (b) Optical spectra of NWs of Fig. 2(a-e).

polycrystalline. Fig. 5d depicts the energy-dispersive X-ray spectroscopy (EDS) spectra of the NWs given in Fig. 5b. There are distinctive peaks for Au, Ag, C and Cu. The elemental analysis showed that the NWs consist for 91% of Au and 9% Ag, whereas the Cu and C peaks are due to the TEM grid and the surfactant, respectively. The presence of Ag in the NWs is attributed to the fact that high pH reaction conditions leads to the reduction of Ag ions. Although the molarities of Ag and Au ions are similar in solution, the concentration of Au in the NWs is much higher. This is due to the fact that most of the AA is consumed in reducing Au^{+3} ions prior to the addition of Ag ions. The molar ratio of Au:AA is 1:1.1 and one unit of AA can donate two electrons.[14] However, when we increased the Au:AA molar ratio to see its effect on the Ag concentration in NWs the yield of NWs was seen to reduce significantly (SEM images not shown).

Fig. 6a depicts the optical spectra of the NWs of Fig. 1. For all samples of NWs, only the high energy plasmon peak is visible (close to 500 nm). Due to the large length and AR of NWs the low-energy plasmon peaks lie beyond the measuring rang of our spectrometer. Similarly, for the NWs of Fig. 2, the higher energy transverse peaks for all samples can be seen around 500 nm (Fig. 6b). For NWs of Fig. 2a the low energy peak is also visible at 875 nm. Compared to Au nanorods of similar AR (AR= 3.5) and polydispersity, the plasmon peak is quite broad. The broadening is due to the polydispersidy in shape. For NWs of Fig. 2b (which have much smaller AR=2.2), there is a shoulder peak at 630 nm which is the low-energy longitudinal plasmon peak. For NWs of Fig. 2c, there is a low energy peak at 710 nm. The rise of the absorption after that peak suggests the presence of another plasmon peak at even lower energy. This is similar to L-shape Au particles where there are two low-energy plasmon peaks.[11] Similarly, a low-energy plasmon peak can be seen for NWs of Fig. 2d at 760nm, and another lower energy peak is expected above 1000 nm. These spectra indicate the presence of multiple plasmon resonances in NWs. Detailed single-particle optical studies are crucial to fully explore all the size and shape dependent plasmon resonances of these NWs.

Conclusions

In summary, we have shown a simple one step method for the high-yield synthesis of Au NWs. We propose that the end-to-end attachment of particles in the growth medium under the influence of electrostatic forces gives rise to the worm-like shape. We further show that the size and the AR of the NWs can be precisely controlled by tuning the concentrations of the reactants. Due to their unique morphology and shape-dependent plasma resonances these NWs can potentially replace conventional nanorods for many applications.

Acknowledgements

This work is part of the Industrial Partnership Programme (IPP) Innovative Physics for Oil and Gas (iPOG) of the Stichting voor Fundamenteel Onderzoek der Materie (FOM), which is supported financially by Nederlandse Organisatie voor Wetenschappelijk Onderzoek (NWO). The IPP iPOG is co-financed by Shell.

Notes and references

[a] Kamerlingh Onnes Laboratory, Niels Bohrweg 2, Leiden University, 2333 CA Leiden, The Netherlands. Email: ruitenbeek@physics.leidenuniv.nl; Phone: +31-71-527-5450, Fax: +31-71-527-5404

[b]Center for Micro and Nano Devices (CMND), Department of Physics, COMSATS Institute of Information Technology, Islamabad, 44000, Pakistan

1 W. Rechberger, A. Hohenau, A. Leitner, J. R. B. Krenn, Lamprecht, F. R. Aussenegg, *Optics Comm.,* 2003, **220**, 137.
2 C. L. Nehl, H Liao. J. H. Hafner, *Nano Lett.,* 2006, **6**, 683.
3 Y-. Ying, S.-S. Chang, C. –L. Lee, C. R. C. Wang, *J. Phys. Chem. B*, 1997, **101**, 6661.
4. J. Aizpurua, P. Hanarp, D. S. Sutherland, M. Käll, G. W. Bryant, F. J. G. de Abajo, *Phys. Rev. Lett.,* 2003, **90**, 057401.
5 S. Eustis, M. A. El-Sayed, *Chem. Soc. Rev.,* 2006, 35, 209.
6 R. D. Averitt, S. L. Westcott, N. J. Halas, *J. Opt. Soc. Am. B,* 1999, **16**, 1824.
7 K. L. Kelly, E. Coronado, L. L. Zhao, J. C. Schatz, *J. Phys. Chem. B*, 2003, **107**, 668.
8 E. S. Kooij , W. Ahmed, H. J. W. Zandvliet, B. Poelsema*, J. Phys. Chem. C,* 2011, **115**, 10321.
9 E. S. Kooij, B. Poelsema, *Phys. Chem. Chem. Phys.,* 2006, **8**, 3349.
10 W. Ahmed, E. S. Kooij, A. van Silfhout, B. Poelsema, *Nano Lett.,* 2009, **9**, 3786.
11 Z.-Y. Zhang, Y.-P. Zhao, *App. Phys. Lett.,* 2006, **89**, 023110.
12 M. Sukharev, J. Sung, K. G. Spears, T. Seideman, *Phys. Rev. B,* 2007, **76**, 184302.
13 H. Husu, R. Siikanen, J. Mäkitalo, J. Lehtolahti, J. Laukkanen, M. Kuittinen, M. Kauranen, *Nano Lett.,* 2012, **12**, 673.
14 B. Nikoobakht, M. A. El-Sayed, *Chem. Mater.,* 2003, **15**, 1957.
15 N. R. Jana, Small, 2005, 1, 875.
16 M. Liu, P. Guyot-Sionnest, *J. Phys. Chem. B,* 2005, **109**, 22192.
17 B. D. Busbee, S. O. Obare, C. J. Murphy, *Adv. Mater*., 2003, **15**, 414.
18 L. J. E. Anderson, Y. –R. Zhen, C. M. Payne, P. Nordlander, J. H. Hafner, *Nano Lett.,* 2013, **13**, 6256.
19 B. K. Jena, C. R. Raj, *J. Phys. Chem. C,* 2007, **111**, 15146.
20 S. Goy-Lopez, E. Castro, P. Taboada, V. Mosquera, *Langmuir,* 2008, **24**, 13186.
21 B. Lim, P. H. C. Camargo, Y. Xia, *Langmuir,* 2008, **24**, 10437.
22 H. Y. Wu, M. Liu, M. H. Huang*, J. Phys. Chem.B,* 2006, **110**, 19291.
23 P. S. Kumar, I. Pastoriza-Santos, B. Rodrıguez-Gonzalez, F. J. G. Abajo, L. M. Liz-Marzan, *Nanotechnology,* 2008, **19**, 015606.
24 H. G. Liao, Y. X. Jiang, Z. Y. Zhou, S. P. Chen, S. G. Sun, *Angew. Chem. Int. Edn,* 2008**, 47**, 9100.
25 W. Ahmed, E. S. Kooij, A. van Silfhout, B. Poelsema, *Nanotechnology,* 2010, **21**, 125605.
26 Y. Huang, W. Wang, H. Liang, H. Xu, *Cryst. Growth Des.*, 2009, **9**, 858.
27 A. Sanchez-Iglesias, I. Pastoriza-Santos, J. Perez-Juste, Rodrıguez-B. Gonzalez, F. J. G. Abajo, L. M. Liz-Marzan *Adv. Mater.,* 2006, **18**, 2529.
28 D. Kim, J. Heo, M. Kim, Y. W. Lee, S. W. Han, *Chem. Phys. Lett.,* 2009, **468**, 245.
29 L. Huang, M. Wang, Y. Zhang, Z. Guo, J. Sun N. Gu, *J. Phys. Chem. C,* 2007, **111**, 16154.
30 E. S. Kooij, W. Ahmed, C. Hellenthal, H. J. W. Zandvliet, B. Poelsema, *Coll. Surf. A: Phys. Eng. Asp.,* 2012, **413**, 231.
31 J. He, Y. Wang, Y. Feng, X. Qi, Z. Zeng, Q. Liu, W. S. Teo, C.L. Gan, H. Zhang, H. Chen, *ACS Nano*, 2013, **7**, 2733.
32 L. Vigderman, E. R. Zubarev, *Chem. Mater.* 2013, 25, 1450.
33 L. Vigderman, E. R. Zubarev, *Langmuir,* 2012, 28, 9034.
34 C. Zhu, H. C. Peng, J. Zeng, J. Liu, Z. Gu, Y. Xia, *J. Am. Chem. Soc.*, 2012, **134**, 20234.
35 H. M. Chen, R. –S. Liu, K. Asakura, L. –Y. Jang, J. –F. Lee *J. Phys. Chem. C,* 2007, **111**, 18550.
36 L. Vigderman, B. P. Khanal, E. R. Zubarev, *Adv. Mater.,* 2012, **24**, 4811.
37 F. Hubert, F. Testard, O. Spalla, *Langmuir*, 2008, **24**, 9219.
38 T. K. Sau, A. L. Rogach, M. Döblinger, J. Feldmann, *Small,* 2011, **7**, 2188.
39 H. –G. Liao, L. Cui, S. Whitelam, H. Zheng, *Science*, 2012, **336**, 1011.